Published in final edited form as:
J Neurochem. 2008 July ; 106(1): 70–82. doi:10.1111/j.1471-4159.2008.05336.x.

Regulation of CB_1 cannabinoid receptor internalization by a promiscuous phosphorylation-dependent mechanism

Tanya L. Daigle[1], **Mary Lee Kwok**[1,2], and **Ken Mackie**[1,2]

[1]Department of Physiology and Biophysics, University of Washington, School of Medicine, Seattle, Washington 98195

[2]Department of Anesthesiology, University of Washington, School of Medicine, Seattle, Washington 98195

Abstract

Agonists stimulate CB_1 receptor internalization. Previous work suggests that the extreme carboxy-terminus of the receptor regulates this internalization – likely through the phosphorylation of serines and threonines clustered within this region. While truncation of the carboxy-terminus (V460Z CB_1) and consequent removal of these putative phosphorylation sites prevents endocytosis in AtT20 cells, the residues necessary for CB_1 receptor internalization remain elusive. To determine the structural requirements for internalization, we evaluated endocytosis of carboxy-terminal mutant CB_1 receptors stably expressed in HEK293 cells. In contrast to AtT20 cells, V460Z CB_1 receptors expressed in HEK293 cells internalized to the same extent and with similar kinetics as the wild-type receptor. However, mutation of serine and/or threonine residues within the extreme carboxy-terminal attenuated internalization when these receptors were expressed in HEK293 cells. These results establish that the extreme carboxy-terminal phosphorylation sites are not required for internalization of truncated receptors, but are required for internalization of full-length receptors in HEK293 cells. Analysis of βarrestin-2 recruitment to mutant CB_1 receptors suggests that putative carboxy-terminal phosphorylation sites mediate βarrestin-2 translocation. This study indicates that the local cellular environment affects the structural determinants of CB_1 receptor internalization. Additionally, phosphorylation likely regulates the internalization of (full-length) CB_1 receptors.

Keywords

cannabinoid; CB1; arrestin; phosphorylation; GPCR; internalization

Introduction

The CB_1 cannabinoid receptor is the primary mediator of the central effects of cannabinoids – a diverse group of compounds including Δ^9-THC, the principal psychoactive constituent of marijuana, a number of synthetic compounds pharmacologically similar to THC, as well as the endogenous cannabinoids. CB_1 receptors are members of the G protein-coupled receptor superfamily of proteins (GPCRs). The cellular consequences of their stimulation include the inhibition of voltage-gated Ca^{2+} channels and cAMP production and the activation of inwardly rectifying K^+ channels and MAP kinases (Howlett and Fleming 1984; Mackie and Hille 1992; Bouaboula et al. 1995; Mackie et al. 1995). In animal models,

Correspondence: Ken Mackie, Department of Psychological and Brain Sciences, Indiana University, 1101 E. 10th St., Bloomington, IN 47405. Tel.: 812-855-2042, FAX: 812-856-7197. kmackie@indiana.edu..

cannabinoid treatment produces a diverse array of behavioral effects including hypolocomotion, hypothermia, antinociception and catalepsy (Howlett et al. 2002).

Behavioral and physiological tolerance to cannabinoids develops rapidly and is primarily mediated by changes in the CB_1 cannabinoid receptor (Bass and Martin 2000). At the cellular level, chronic cannabinoid treatment has generally been associated with a decrease in CB_1 receptor function and/or binding sites (Breivogel et al. 1999; Breivogel et al. 2003). Concomitant with these findings, CB_1 receptors are desensitized and internalized following protracted agonist exposure (Rinaldi-Carmona et al. 1998; Hsieh et al. 1999; Jin et al. 1999; Coutts et al. 2001; Kouznetsova et al. 2002). Thus, CB_1 receptor desensitization and internalization have consistently been implicated as two potential cellular correlates underlying the development and maintenance of behavioral tolerance (Martin et al. 2004). Therefore, identifying the molecular mechanisms regulating CB_1 receptor internalization will be critical for understanding the implications of chronic cannabis use as well as assessing the clinical potential of cannabinoid-based therapies.

Studies involving the prototypic β_2-adrenergic receptor have significantly advanced our knowledge of the regulatory mechanisms governing GPCR internalization (Lefkowitz 2004). Agonist stimulation of GPCRs results in the activation of heterotrimeric G-proteins and subsequent dissociation of their α and $\beta\gamma$ subunits. Typically, the $\beta\gamma$ subunit of the activated G-protein then recruits members of the G-protein coupled receptor kinase family of proteins (GRKs) resulting in the phosphorylation of specific serine and threonine residues in the carboxy-terminus of the GPCR. Binding of the multi-functional βarrestin proteins to the phosphorylated receptors uncouples them from G-proteins and attenuates their signaling (desensitization). βarrestin also promotes clathrin-dependent internalization of GPCRs through the scaffolding of essential endocytic adaptor proteins (reviewed in Refs. (Claing et al. 2002; Gainetdinov et al. 2004)).

However, not all GPCRs are desensitized and internalized through the mechanisms implicated for the β_2-adrenergic receptor, thus the process needs to be examined for each GPCR (Smyth et al. 2000; Chen et al. 2004). Recent studies have shed some light unto the mechanisms regulating agonist-induced internalization of the CB_1 receptor (Leterrier et al. 2004; Leterrier et al. 2006; McDonald et al. 2006; Martini et al. 2007) and also have provided a physiological framework for the study of CB_1 receptor internalization in the context of neurodevelopment and drug tolerance (Berghuis et al. 2007; Tappe-Theodor et al. 2007). However, the basic structural requirements for agonist-induced internalization at the receptor level have yet to be elucidated. The extreme carboxy-terminal tail of the CB_1 receptor has previously been implicated as a central mediator of agonist-induced internalization of the receptor in AtT20 cells (Hsieh et al. 1999). This region (residues 460–473 of the rat CB_1 receptor) contains a cluster of six serines and threonines, which may be putative GRK phosphorylation sites. While removal of these residues by truncation of the receptor prevents internalization, the contribution of these sites individually to CB_1 receptor endocytosis has yet to be determined.

The aim of the present study was to determine which of the putative phosphorylation sites in the carboxy-terminal tail of the CB_1 receptor regulate internalization following agonist activation. We used HEK293 cells stably expressing CB_1 receptors to investigate the contributions of these residues to the kinetics and extent of CB_1 receptor internalization. We found that the putative carboxy-terminal phosphorylation sites facilitated internalization in a graded fashion. Our results strongly suggest that the non-phosphorylated extreme carboxy-terminus restrains internalization of the CB_1 receptor and further indicate that promiscuous phosphorylation within this region relieves this inhibition.

Experimental Procedures

Drugs and Reagents

CP 55,940 ((−)-*cis*-3-[2-hydroxy-4-(1,1-dimethylheptyl)phenyl]-*trans*-4-(3-hydroxypropyl) cyclohexanol) and SR141716A (4-chlorophenyl)-1-(2,4-dichloro-phenyl)-4-methyl-*N*-(piperidin-1-yl)-1*H*–pyrazole-3-carboxamide) were provided by the National Institute of Drug Abuse Drug Supply Program (RTI, Research Triangle Park, NC). WIN 55,212-2 (R)-(+)-[2,3-dihydro-5-methyl-3-(4-morpholinylmethyl)pyrrolo [1,2,3-de)-1,4-benzoxazin-6-yl]-1-napthalenylmethanone was purchased from Sigma-Aldrich (St. Louis, MO). HU-210 (11-hydroxy-Δ^8-THC dimethylheptyl) was a gift from Raphael Mechoulam (Hebrew University).

Generation of mutant CB_1 receptor constructs

CB_1 receptor mutants T461A/S463A, S465A/T466A, T468A/S469A, T461A–T466A and T461A–S469A were made using a modified QuikChange PCR strategy (Stratagene, La Jolla, CA). Full-length rat CB_1, with an amino-terminal pplssHA (prolactin signal sequence and hemagglutinin epitope) tag (Andersson et al. 2003) in pcDNA3.0 (Invitrogen, Carlsbad, CA), was used as a template to generate the T461A/S463A, S465A/T466A and T468A/S469A mutant constructs. The T461A/S463A construct was used as template to make the T461A–T466A plasmid and the T461A/T466A construct was used as a template to generate the T461A–S469A mutant. In all cases the single base modifications introduced a unique restriction site that was used for screening purposes. Integrity of the entire coding region for all constructs was verified by sequencing. The A470Z, V464Z, and V460Z CB_1 receptor mutants were generated by PCR using full-length rat CB_1 in pcDNA3.0 as template as previously described (Hsieh et al. 1999).

Cell Culture and Transfection

HEK293 and AtT20 cells were grown in DMEM containing 10% fetal bovine serum and penicillin/streptomycin (GIBCO, Carlsbad, CA) at 37°C in 5% CO_2. Transfections were performed in 35-mm dishes with 2–5 μg of the appropriate plasmid and either Lipofectamine 2000 (Invitrogen, Carlsbad, CA) for HEK293 cells or Superfect (Qiagen, Valencia, CA) for AtT20 cells. Stable cell lines of all constructs were generated by selection in 0.8–1.2 mg/ml Geneticin (G418; Invitrogen, Carlsbad, CA). G418-resistant colonies were evaluated for the surface expression of CB_1 receptors by live cell immunostaining using an antibody directed towards the amino-terminal extracellular HA epitope tag (Covance, Berkeley, CA) and a fluorescein isothiocyanate (FITC) secondary antibody (Jackson ImmunoResearch Laboratories Inc., West Grove, PA). Clones expressing uniform and moderate to high levels of CB_1 receptors were expanded and used for subsequent experiments. The relative levels of expression of CB_1 receptors between the mutant and wild-type lines were not significantly different. A minimum of two stable cell lines were generated and analyzed for each mutant CB_1 receptor.

Quantitative Internalization Assay

Agonist-induced internalization of CB_1 receptors was assessed in HEK293 cells using a previously described method (Daigle et al. 2008). Briefly, HEK293 cells stably expressing wild-type or mutant CB_1 receptors were seeded onto poly-D-lysine coated 96-well plates and grown until 90% confluent. Before drug treatment, plates were washed once in HEPES-buffered saline (HBS; 130 mM NaCl, 5.4 mM KCl, 1.8 mM $MgCl_2$ and 10 mM HEPES, pH 7.4) containing 1.0 mg/ml bovine serum albumin (BSA; Sigma-Aldrich, St. Louis, MO). Cells were then incubated in the appropriate drug solution supplied in HBS containing 1.0 mg/ml BSA. At the end of the incubation, the plate was placed on ice and cells were

immediately fixed in 4% paraformaldehyde (PFA) for 30 min at room temperature. PFA alone (in the absence of detergent) does not cause substantial membrane permeabilization in this cell model (Daigle et al. 2008). Following fixation, cells were washed 5X for 30 min in phosphate-buffered saline (PBS; 137 mM NaCl, 10 mM NaH_2PO_4 and 2.7 mM KCl, pH 7.4) and blocked for 90 min in LI-COR Odyssey Blocking Buffer® (LI-COR Biosciences, Lincoln, Nebraska) at room temperature. Cells were then incubated overnight at 4°C with a monoclonal anti-HA antibody (1:100; Covance, Berkeley, CA). The following day, cells were washed 5X for 30 min in Tris-buffered saline containing 0.05% Tween-20 (TBST; 137 mM NaCl and 10 mM Tris, 0.05% Tween-20, pH 7.4) and then incubated with an IRDye 800 conjugated anti-mouse IgG (1:800; Rockland Immunochemicals, Inc., Gilbertsville, PA). Plates were washed 5X in TBST for 30 min and the immunocomplex was visualized on a LI-COR Odyssey according to the manufacturer's instructions.

Quantitative Measurement of ERK1/2 Phosphorylation

CB_1 receptor-mediated activation of ERK1/2 in HEK293 cells was assessed as described previously (Daigle et al. 2008). In brief, HEK293 cells stably expressing wild-type or mutant CB_1 receptors were seeded onto poly-D-lysine coated 96-well plates and grown until 90% confluent at 37°C in 5% CO_2. Cells were serum starved overnight in DMEM containing only penicillin/streptomycin the day before the experiment. Drug treatments were performed as described in the preceding section. Following drug treatment, cells were fixed with 4% paraformaldehyde for 15 min on ice and then an additional 45 min at room temperature. After fixation, cellular membranes were permeabilized with 100% methanol at −20°C for 30 min and cells were then blocked for 1.5 hr in Tris-buffered saline (TBS; 137 mM NaCl and 10 mM Tris, pH 7.40) containing 5.0 mg/ml BSA. Following blocking, cells were incubated overnight at 4°C with a phospho-specific ERK1/2 antibody (1:200; Cell Signaling Technologies Inc., Danvers, MA). Excess primary antibody was removed with 5X washes in TBST over 1.5 hr and bound antibody detected with an IRDye 800 conjugated anti-rabbit IgG (1:800; Rockland, Gilbertsville, PA). After incubation with secondary antibody, cells were washed 5X in TBST for 1.5 hr and immunofluorescence was visualized on the LI-COR Odyssey.

Immunocytochemistry, Microscopy and βarrestin-2 Recruitment

CB_1 receptor distribution in both AtT20 and HEK293 stable cell lines was evaluated using a previously described method to image surface and intracellular receptors (Hsieh et al. 1999; Kearn et al. 2005). Briefly, cells were seeded onto poly-D-lysine coated glass coverslips, washed 1X in HBS and incubated with the specified drug. Following drug application, cells were immediately fixed with 4% paraformaldehyde for 30 min, washed 5X with PBS and blocked for 1 hr in PBS containing 5% donkey serum and 0.1% saponin (to permeabilize cellular membranes). Cells were then incubated overnight at 4°C with a monoclonal mouse anti-HA antibody (1:1000; Covance, Berkeley, CA). Following 5X washes in PBS, bound primary antibody was detected with a FITC anti-mouse IgG antibody (1:150; Jackson Immunoresearch Laboratories, West Grove, PA). Coverslips were washed 2X in PBS, 2X in PB (10 mM NaH_2PO_4 and 2.7 mM KCl. pH 7.4), 1X in water, dried and mounted in Vectashield (Vector Laboratories, Burlingame, CA). Images (1024 × 1024 pixels) were obtained on a Leica SP1/MP confocal microscope by the use of a 100X objective. Detection of FITC fluorescence was done by excitation with the 488 nm laser.

For βarrestin-2 recruitment studies, HEK293 cells were transiently transfected with constructs encoding either wild-type or mutant CB_1 receptors and either an RFP- or GFP-tagged βarrestin-2 fusion protein at a ratio of 1 μg of arrestin DNA: 5–10 μg of CB_1 receptor DNA. The GFP-tagged βarrestin-2 construct (a gift from Marc Caron) was modified using a standard molecular biology approach to insert the red fluorescent protein in place of the GFP

(Campbell et al. 2002). Superfect (Qiagen, Valencia, CA) was utilized for transfection of AtT20 cells while Lipofectamine 2000 (Invitrogen, Carlsbad, CA) was used for HEK293 cells. The manufacturer's recommendations were followed for both transfection reagents. Following transfection, cells were plated onto coverslips and the experiment was performed 24 hr post-transfection. CB_1 receptor expression was detected using the above-mentioned HA antibody and protocol. Cells expressing moderate to high levels of CB_1 receptors and low to moderate levels of βarrestin-2 were selected for analysis. Images (1024 × 1024) were obtained on a Leica SP1/MP confocal microscope by the use of a 100X objective and 2X zoom, resulting in a pixel size of 50 nm. Co-detection of RFP or GFP and FITC or Texas Red fluorescence was done by excitation with 488 and 561 nm lasers.

Quantitative and Statistical Analysis of Internalization, ERK1/2 Phosphorylation and βarrestin-2 Recruitment

For the internalization studies, the percentage of cell surface receptors remaining was determined by initially calculating the mean integrated intensity values for each drug at the individual time points. Background subtraction was not evaluated for the individual experiments; however, the non-specific binding for the HA antibody was determined to be 5–10% in wild-type HEK293 cells. Final mean integrated intensity values were normalized to the mean integrated intensity values for the no drug treated controls and these data are represented as the mean ± SEM. Extent of internalization curves were fit by nonlinear regression. The half-life of decay ($t_{1/2}$) was calculated by fitting the data to a single-phase exponential decay model. For the ERK1/2 phosphorylation studies, percent maximal response for ERK1/2 activation was calculated by defining basal to be the phosphorylation level at time zero and setting the maximal peak phosphorylation to 100%. Statistical significance with respect to the extent of internalization and maximal ERK1/2 activation was calculated with a one-way ANOVA (Dunnett's post-test, 99% CI; $^{**}p < 0.01$, $^{*}p < 0.05$) for multiple groups or an unpaired Student's t-test for only two groups. To quantify βarrestin-2 recruitment, the membrane to cytosolic ratio of fluorescence in the 561 nm channel was calculated by region-specific analysis of averaged intensity values using MetaMorph software (Molecular Devices, Downingtown, PA). These data are represented as the mean ± SEM. Rate of recruitment curves were fit by nonlinear regression. The half-life of recruitment ($t_{1/2}$) was calculated by fitting the data to a one-phase exponential association. Statistical significance was calculated with a one-way ANOVA or unpaired t-test. All graphs and statistical analyses were generated using GraphPad Prism 4.0 software (Hearne Scientific Software, Chicago, IL).

Results

Removal of the extreme carboxy-terminus (V460Z mutation) of the CB_1 receptor has been shown previously to prevent WIN 55,212-2-induced internalization in AtT20 cells (Hsieh et al. 1999). Consistent with our earlier results, after a 30 min treatment with a maximally efficacious concentration of the CB_1 agonist, WIN 55,212-2 (1 μM), V460Z CB_1 receptors stably expressed in AtT20 cells remained at the cell surface (Fig. 1A, g) while wild-type CB_1 receptors were rapidly endocytosed (Fig. 1A, b). To preclude the possibility of agonist-specific endocytosis, internalization of V460Z CB_1 receptors was evaluated using a maximally efficacious concentration of a structurally distinct CB_1 agonist, CP 55,940 (100 nM) (Fig. 1A). As for WIN 55,212-2, little internalization of V460Z CB_1 receptors was observed with CP 55,940 stimulation (Fig. 1A, i) whereas in cells expressing wild-type CB_1 receptors notable internalization was evident (Fig. 1A, d). Agonist-induced internalization of wild-type CB_1 receptors was prevented in the presence of 1 μM of the CB_1 antagonist, SR141716A (Fig. 1A, c, e) and additionally, SR141716A had no affect on the surface expression of V460Z CB_1 receptors (Fig. 1A, h, j). These observations are consistent with

our previous findings and firmly establish that the V460Z truncated CB_1 receptor does not undergo substantial agonist-induced internalization when stably expressed in AtT20 cells.

Phosphorylation in the carboxy-terminus of many GPCRs is a well-described regulatory mechanism for both internalization and desensitization (Claing et al. 2002; Gainetdinov et al. 2004). βarrestin's in particular have been implicated as key mediators of endocytosis via their direct interaction with the phosphorylated receptor. Since V460Z CB_1 receptors fail to undergo internalization in AtT20 cells, we examined whether βarrestin recruitment to the plasma membrane following agonist activation was reduced in cells expressing this truncated receptor. βarrestin-2 translocation in AtT20 cells transiently expressing GFP-tagged βarrestin-2 and either wild-type or V460Z CB_1 receptors was evaluated by confocal imaging (Fig. 1B). In the absence of agonist stimulation, βarrestin-2-GFP was expressed throughout the cell (Fig. 1B, a, c). Agonist activation of wild-type CB_1 receptors caused a rapid redistribution of βarrestin-2-GFP (Fig. 1B, b), with large βarrestin-2 containing clusters evident at the plasma membrane following 100 nM WIN 55,212-2 treatment (Fig. 1B, b). These observations are consistent with our recent findings describing βarrestin-2-RFP recruitment to wild-type CB_1 receptors in HEK293 cells (Daigle et al. 2008). We then evaluated βarrestin-2-GFP translocation in cells expressing V460Z CB_1 receptors. In contrast to wild-type CB_1 receptors, no agonist-induced redistribution of βarrestin-2-GFP was evident in cells expressing the truncated receptor (Fig. 1B, d). Taken together, these results strongly suggest that the extreme carboxy-terminus of the CB_1 receptor is required for agonist-induced internalization and βarrestin-2 recruitment in AtT20 cells.

While AtT20 cells are advantageous when a neuronal-like cell line is needed, HEK293 cells are much more commonly used when studying receptor trafficking. Therefore we examined whether the extreme carboxy-terminus of CB_1 was required for agonist-induced internalization in HEK293 cells. Wild-type and V460Z CB_1 receptors were stably expressed in HEK293 cells and receptor trafficking was initially assessed by confocal imaging (Fig. 2A). Surprisingly, the trafficking of V460Z CB_1 receptors in HEK293 cells was significantly different from that in AtT20 cells (Fig. 2). In HEK293 cells, both wild-type and V460Z CB_1 receptors were rapidly internalized following 100 nM CP 55,940 treatment (Fig. 2A, a–b, d–e). Agonist-induced internalization of either receptor was prevented by the addition of 1 μM SR141716A (Fig. 2A, c, f). Rapid internalization of V460Z CB_1 receptors was consistently observed in a multitude of monoclonal cell populations over a range of expression levels and also when transiently expressed (data not shown), thus it was a robust observation. The ability of V460Z CB_1 receptors to be internalized was also evaluated in a quantitative fashion. Significant internalization of V460Z CB_1 receptors was observed (46.3 ± 1.2% surface receptors at 120 min) relative to wild-type CB_1 receptors (53.7 ± 2.6% surface receptors at 120 min) following treatment with 100 nM CP 55,940 (Fig. 2B). Furthermore, the rate of internalization for V460Z CB_1 receptors was not significantly different from that for wild-type CB_1 (wild-type $t_{1/2}$ = 18.9 ± 5.4 min versus V460Z $t_{1/2}$ = 29.5 ± 4.8 min; $p = 0.27$), although there was a trend toward slower internalization for the mutant. It has been previously shown that truncation of the last ten (V464Z) or last four (A470Z) amino acid residues of the CB_1 receptor is without affect on WIN-induced internalization in AtT20 cells (Hsieh et al. 1999). Consistent with previous work, rapid internalization of A470Z and V464Z CB_1 receptors (50.6 ± 2.7% surface receptors at 120 min for A470Z and 49.1 ± 1.7% surface receptors at 120 min for V464Z) was observed (Fig. 2B). To preclude the possibility of agonist-specific internalization, the extent of internalization of V460Z CB_1 receptors was evaluated using two additional agonists, WIN 55,212-2 (1 μM) and HU-210 (100 nM). In agreement with the CP 55,940 results, both receptors internalized to a similar extent in the presence of either agonist (WIN: 46.9 ± 1.8% surface receptors at 120 min for wild-type versus 48.2 ± 0.4% surface receptors at 120 min for V460Z; HU-210: 47.8 ± 1.7% surface receptors at 120 min for wild-type versus 49.9 ±

0.2% for V460Z) and without significantly different kinetics between mutant and wild-type receptors (WIN: wild-type $t_{1/2}$ = 3.2 ± 0.26 min versus V460Z $t_{1/2}$ = 3.87 ± 0.27 min; HU-210: wild-type $t_{1/2}$ = 11.6 ± 2.7 min versus V460Z $t_{1/2}$ = 26.5 ± 5.8 min; p = 0.24 for WIN and 0.14 for HU-210) (Fig. 1C). Thus, in contrast to the near complete absence of agonist-induced internalization of V460Z receptors in AtT20 cells, truncated V460Z CB_1 receptors internalize to a similar extent and at a similar rate to wild-type CB_1 when stably expressed in HEK293 cells.

Truncation of the CB_1 receptor at residue 460 removes the end of the cytoplasmic tail and with it, six putative regulatory serine and threonine phosphorylation sites. Therefore, we next examined whether these residues were required for internalization of full-length CB_1 receptors in HEK293 cells. Full-length mutant versions of the CB_1 receptor in which two (T461A/S463A, S465A/T466A and T468A/S469A), four (T461A–T466A), or all six (T461A–S469A) serines and/or threonines were mutated to alanine were generated and the extent of 100 nM CP 55,940-induced internalization over time was determined for each mutant (Fig. 3). Rapid internalization of T461A/S463A, S465A/T466A and T468A/S469A CB_1 receptors (all with four putative phosphorylation sites remaining) was observed (for example at 120 min, the percent of surface receptors on average for mutant receptors was 66 ± 1.4% relative to 57.9 ± 4.9% surface receptors for wild-type) (Fig. 3B). Interestingly, the rate of S465A/T466A ($t_{1/2}$ = 4.5 ± 0.7 min) and T468A/S469A ($t_{1/2}$ = 6.2 ± 0.9 min) CB_1 receptor internalization was significantly faster ($p<0.01$) than for T461A/S463A ($t_{1/2}$ = 15.4 ± 1.9 min) receptors, suggesting a potential modulatory role of these latter two residues on the kinetics of endocytosis. In contrast, the character of T461A–T466A and T461A–S469A CB_1 receptor (with two or no putative phosphorylation sites remaining, respectively) endocytosis was markedly different (Fig. 3C). While the rate of internalization was similar for these mutant receptors (T461A–T466A $t_{1/2}$ = 14.02 min, T461A–S469A ($t_{1/2}$ = 12.41 min, wild-type $t_{1/2}$=13.2 min), the extent of internalization was significantly attenuated at all time points tested for T461A–S469A CB_1 receptors and at time points ≥ 30 min for T416A–T466A CB_1 receptors (91.8 ± 4.5 % surface receptors on average at 120 min) (Fig. 3C). Internalization of representative mutated receptors from each group (two, four or all six putative phosphorylation sites mutated) was next visualized by confocal microscopy (Fig. 4A). In the absence of drug treatment, wild-type, T461A/S463A, T461A–T466A, and T461A–S469A CB_1 receptors were predominantly enriched at the cell surface (Fig. 4A, a, d, g, j). Consistent with the quantitative results, rapid internalization of only wild-type and T461A/S463A CB_1 receptors was evident after 100 nM CP 55,940 stimulation (Fig. 4A, b, e). Little internalization of T461A–T466A and T461A–S469A CB_1 receptors was detectable (Fig. 4A, h, k). Interestingly, a significant fraction of T461A–S469A CB_1 receptors were present in the cytosol prior to drug treatment (Fig. 4A, j). Recent studies have suggested that the intracellular accumulation of CB_1 receptors may be a result of the constitutive cycling of receptors in the absence of agonist (Leterrier et al. 2004; Leterrier et al. 2006). Therefore we evaluated wild-type and T461A–S469A CB_1 receptor trafficking during sustained treatment with SR141716A (Fig. 4B). No increase in cell surface CB_1 receptors was evident following prolonged SR141716A treatment, suggesting that the intracellular pool of receptors was not a consequence of constitutive activity (Fig. 4B). Our results thus far suggest in HEK293 cells that the extreme carboxy-terminus of the CB_1 receptor is not required for endocytosis. However, phosphorylation of this domain contributes to endocytosis of native (full-length) CB_1 receptors as their internalization is attenuated when four or more putative phosphorylation sites in this domain are mutated to alanine. Furthermore, there is a graded effect on the extent of agonist-induced endocytosis whereby internalization proceeds normally when at least four putative phosphorylation sites are available, is significantly reduced when two remain, and is essentially absent when all six are removed.

It is well established that the CB_1 cannabinoid receptor internalizes via clathrin-coated pits in heterologous expression systems (Hsieh et al. 1999; Keren and Sarne 2003). Because of the paradoxical internalization results of the V460Z mutant compared to the phosphorylation site mutants, we next examined whether V460Z receptors internalize via the canonical, clathrin-dependent, pathway. We used a hypertonic sucrose solution (450 mM) to selectively disrupt clathrin-coated pit formation (Heuser and Anderson 1989), a strategy utilized in previous studies (Hsieh et al. 1999; Keren and Sarne 2003) (Fig. 5). Cells expressing wild-type or mutant CB_1 receptors were treated with sucrose for 15 min and then stimulated for 45 min with an efficacious concentration of CP 55,940 (20 nM) diluted in sucrose containing solution. As expected, blockade of clathrin-dependent internalization by sucrose significantly attenuated (57 ± 0.8% of surface receptors remaining for control versus 104 ± 0.3% remaining with sucrose) agonist-induced wild-type CB_1 receptor endocytosis (Fig. 5A). Similarly, the extent of V460Z, T461A/S463A, S465A/T466A, T468A/S469A and T461A–T466A CB_1 receptor internalization was significantly reduced in the presence of sucrose with an average of 100 ± 1.4% of receptors remaining on the surface across the different cell lines (Fig. 5A, B). These data are consistent with a clathrin-dependent mechanism and suggest that truncated and phosphorylation site CB_1 mutants do not internalize via a previously uncharacterized pathway following agonist activation.

The loss of phosphorylation sites in the extreme carboxy-terminus of the CB_1 receptor might inhibit its internalization by reducing the recruitment of βarrestin to the plasma membrane following receptor activation by agonist. To test this hypothesis, we evaluated βarrestin-2 translocation in HEK293 cells transiently expressing βarrestin-2-RFP and either wild-type or mutant CB_1 receptors by confocal imaging (Fig. 6). At steady state, CB_1 receptors are localized to the plasma membrane and within the cytosol, while βarrestin-2-RFP is expressed uniformly throughout the cytosol in HEK293 cells (Fig. 6A, a–b, f–g, k–l, p–q). Consistent with previous observations (Daigle et al. 2008), βarrestin-2-RFP was recruited to the plasma membrane following 100 nM CP 55,940 stimulation in cells expressing wild-type CB_1 receptors (Fig. 6A, d; denoted by arrows). Co-localization of βarrestin-2-RFP clusters and wild-type CB_1 receptors was evident at the cell surface in stimulated cells (Fig. 6A, e). Quantitative analysis of βarrestin-2-RFP recruitment to wild-type CB_1 receptors revealed a two-fold increase in the membrane/cytosolic fluorescence ratio (0.9 ± 0.08 at time zero versus 1.8 ± 0.19 at 15 min) indicative of an increase in membrane-associated βarrestin-2-RFP (Fig. 6B). Similarly, in cells expressing V460Z and T461A/S463A CB_1 receptors, a pronounced redistribution of βarrestin-2-RFP was evident with agonist stimulation (Fig. 6A, i, n) and resulted in the co-localization of some mutant receptors with βarrestin-2-RFP at the membrane (Fig. 6A, j, o). Similar to wild-type, a two-fold increase in the membrane/cytosolic fluorescence ratio was observed when recruitment was quantitatively evaluated (1.8 ± 0.1 at 15 min for V460Z, 1.7 ± 0.1 at 15 min for T461A/S463A) (Fig. 6C). Additionally, robust βarrestin-2-RFP recruitment was apparent in cells expressing S465A/T466A or T468A/S469A CB_1 receptors (1.5 ± 0.08 at 15 min for S465A/T466A and 1.6 ± 0.1 at 15 min for T468A/S469A) (Fig. 6C). Interestingly, while the extent of βarrestin-2-RFP recruitment was similar between wild-type and mutant receptors, the rates differed. Significantly, wild-type CB_1 receptors recruited βarrestin-2-RFP more rapidly ($t_{1/2}$ = 0.71 min) than V460Z ($t_{1/2}$ = 2.46 min), T461A/S463A ($t_{1/2}$ =2.76 min), S465A/T466A ($t_{1/2}$ = 2.65 min) and T468A/S469A ($t_{1/2}$ = 6.2 min) CB_1 receptors under the same conditions. In contrast, activation of T461A–T466A or T461A–S469A CB_1 receptors expressed at similar levels, failed to stimulate detectable βarrestin-2-RFP translocation over the time course evaluated (for example, membrane to cytosolic ratios of 1.1 ± 0.06 at 15 min for T461A–S466A and 1.0 ± 0.06 for T461A–S469A) (Fig. 6A, r–t and D). Collectively, these results suggest that there is a correlation between receptor-mediated recruitment of βarrestin and the extent of agonist-induced internalization of mutant CB_1 receptors.

Both *in vitro* and *in vivo* studies have demonstrated that cannabinoids activate CB_1 receptors to stimulate MAP kinases of the extracellular signal-regulated kinase (ERK) family (Bouaboula et al. 1995; Derkinderen et al. 2003; Rubino et al. 2004). Furthermore, it has recently been demonstrated in HEK293 cells (Daigle et al. 2008) that the time course of CB_1 receptor-mediated activation of ERK1/2 is primarily determined by CB_1 receptor desensitization – a process which requires βarrestin (Jin et al. 1999; Kouznetsova et al. 2002). In light of these observations, the functional consequences on ERK1/2 signaling associated with differences in βarrestin recruitment and receptor internalization of all the mutant CB_1 receptors were examined. The kinetics of ERK1/2 phosphorylation was evaluated following agonist stimulation (100 nM CP 55,940) of wild-type or mutant CB_1 receptors stably expressed in HEK293 cells (Fig. 7). Agonist stimulation of wild-type CB_1 resulted in the transient phosphorylation of ERK1/2 with peak activation at 5–7 min followed by rapid decay ($t_{1/2}$ = 1.7 min) to near basal levels (Fig. 7A,B). While both wild-type and internalization-competent or -deficient mutant CB_1 receptors activated ERK1/2 to a similar extent (2–3 fold activation over basal; supplemental Fig. 1C) and the levels of total ERK1/2 were not significantly different in each line relative to cells expressing wild-type CB_1 receptors (supplemental Fig. 1B), sustained ERK1/2 phosphorylation was evident at time points ≥ 20 min (for example at 45 min, percent of peak activation on average for mutants was 39.8 ± 4.1 relative to 16.2 ± 1.2% of peak for wild-type) with mutant CB_1 receptor stimulation (Fig. 7B–E). Significantly, there was no correlation between the internalization phenotype of the individual mutant receptors and sustained ERK1/2 activation suggesting that internalization does not modulate ERK1/2 phosphorylation. The residual ERK1/2 phosphorylation evident with the mutant CB_1 receptors may potentially reflect a deficiency in receptor uncoupling.

Discussion

The principal finding of this study is that the extreme carboxy-terminus of the CB_1 receptor is not simply required for its agonist-induced endocytosis in HEK293 cells but rather functions as an inhibitor of receptor internalization. Using HEK293 cells stably expressing CB_1 receptors, we found that truncation of CB_1 at residue 460 was without effect on the rate or extent of agonist-induced internalization. In contrast, mutation of four or more putative phosphorylation sites within this distal region of the receptor dramatically reduced the extent of clathrin-dependent internalization. Interestingly, the degree of βarrestin recruitment to agonist-activated receptors correlated with the extent of internalization. Together, these results suggest that phosphorylation of the CB_1 receptor in the distal carboxy-terminus regulates rapid endocytosis by alleviating an inhibitory interaction that normally prevents internalization of agonist-activated full-length receptors.

In contrast to the results obtained with HEK293 cells, truncation of the distal carboxy-terminus of CB_1 receptors expressed in AtT20 cells prevented its internalization. This agonist-induced internalization of V460Z CB_1 receptors in HEK293 cells was not a result of agonist-specific internalization since three distinct, efficacious CB_1 receptor agonists (CP 55,940, WIN 55,212-2 and HU-210) produced substantial internalization of V460Z receptors. In addition, significant endocytosis of V460Z CB_1 receptors was evident in all monoclonal HEK293 cell lines and when transiently expressed, thus the differences between HEK293 and AtT20 cells are unlikely to be due to differences in expression level. Like CB_1 receptor internalization reported previously, internalization of V460Z CB_1 receptors in HEK293 cells likely proceeds via a clathrin pathway, as endocytosis was prevented by hypertonic sucrose. Collectively these data strongly suggest that individual cell lines vary considerably in their ability to support and regulate GPCR internalization. This likely reflects different cellular components in these cell lines. Interestingly, the recently identified CB_1 receptor interacting protein, CRIP1a, is expressed in AtT20 cells but not in HEK293

cells and interacts exclusively with the distal carboxy-terminus of the CB_1 receptor (Niehaus et al. 2007). One intriguing possibility is that CRIP1a may be directly (through the physical interaction with CB_1) or indirectly (through PDZ interactions) involved in the regulation of CB_1 receptor internalization. If this were the case, the differences in receptor trafficking between cell lines may be a reflection of the differential expression of this protein.

Our results with CB_1 receptor phosphorylation site mutants expressed in HEK293 cells strongly support the notion that the distal carboxy-terminus constitutes an important regulatory domain for agonist-induced internalization. A graded effect on clathrin-dependent CB_1 receptor internalization was evident with the successive mutation of putative phosphorylation sites within this region. When two phosphorylation sites were mutated (T461A/S463A, S465A/T466A or T468A/S469A), internalization proceeded normally. However, internalization was significantly reduced when four sites were mutated (T461A–T466A) and essentially abolished (>96% of receptors remained at the surface) when all six sites (T461A–S469A) were mutated. Taken together, these data strongly suggest that phosphorylation of discrete residues in the carboxy-tail is not necessary for internalization, but rather, promiscuous phosphorylation of any serine and/or threonine residue within this region contributes equally to promote endocytosis. These data also suggest that a minimum of three phosphorylation events must occur for CB_1 receptors to internalize to the same rate and extent as wild-type CB_1 receptors. A similar, non-discrete phosphorylation in the carboxy-terminus has been previously suggested to control the trafficking of at least one other GPCR, the thrombin receptor PAR1 (Hammes et al. 1999). Furthermore, since CB_1 truncation at residue 460 in HEK293 cells was without effect on internalization, one function of the distal tail of the CB_1 receptor may be to prevent its endocytosis, possibly via protein-protein interactions. A corollary of this hypothesis is that V460Z CB_1 receptors may internalize via a phosphorylation-independent mechanism.

The current study is the first to correlate βarrestin recruitment, a robust indicator of GPCR activation (Barak et al. 1997), with CB_1 cannabinoid receptor internalization. Consistent with our previous results (Daigle et al. 2008), we found that βarrestin-2 was rapidly recruited (within 1–5 min) to the plasma membrane following CB_1 receptor activation in both AtT20 and HEK293 cells. Since the internalization domain of the CB_1 receptor (residues 460–473) is a likely candidate for mediating βarrestin-2 recruitment, we evaluated βarrestin-2 translocation to internalization-competent (V460Z, T461A/S463A, S465A/T466A and T468A/S469A) and – deficient (T461A–T466A and T461A–S469A) CB_1 receptors in HEK293 cells. Consistent with its central role in endocytosis, we found that all of the internalization-competent CB_1 receptors caused βarrestin-2 redistribution to the same extent as wild-type receptors. However, the rate of βarrestin-2 recruitment to internalization-competent (V460Z, T461A/S463A, S465A/T466A and T468A/S469A) mutant CB_1 receptors was 3–6 times slower than for wild-type receptors. We also found that βarrestin-2 recruitment to internalization-incompetent CB_1 receptors was essentially absent, even with sustained agonist stimulation. One interpretation of these results is that CB_1 receptor internalization is necessary to recruit βarrestin (e.g., βarrestin is being recruited to clathrin-coated pits, and not directly to CB_1 receptors), so βarrestin recruitment is attenuated when internalization of CB_1 receptors is reduced. This hypothesis is also supported by the observation that the non-internalizing CB_1 receptor mutant, D146N, does not recruit βarrestin (M.L.K. and K.M., unpublished observations) (Roche et al. 1999). Arrestin recruitment is not merely a function of carboxy-terminal CB_1 receptor phosphorylation, as it is maintained in the V460Z mutant. A less likely possibility is that mutation of the carboxy-terminus induces structural changes in the receptor resulting in a lower affinity state for βarrestin binding. These data also indirectly suggest that βarrestin recruitment is important for CB_1 receptor internalization. Additional evidence for this notion is that the dominant

negative βarrestin (319–418) prevents CB_1 receptor internalization (M.L.K. and K.M., unpublished results).

Our results are reminiscent of earlier reports from the opioid receptor trafficking field. Murray et al. reported cell-type specific differences in the trafficking of a truncated δ-opioid receptor (Murray et al. 1998). In particular, they reported that the degree of internalization of a truncated δ-opioid receptor (DOR344T) was profoundly different when expressed in HEK293 compared to CHO cells. Interestingly, DOR344T receptors were not phosphorylated following agonist activation suggesting phosphorylation-independent internalization. In a subsequent study, Whistler et al. examined whether phosphorylation sites within the truncated region were required for endocytosis of full-length receptors (DOR5A mutation) (Whistler et al. 2001). As in our study, they found that phosphorylation was required for internalization of full-length receptors, but was not necessary for endocytosis of truncated receptors. They attributed the differences in trafficking to a “brake” mechanism that prevented endocytosis of full-length δ-opioid receptors and was relieved by phosphorylation in the carboxy-terminal tail of the receptor. Interestingly, they also noted a significant correlation between receptor-mediated recruitment of βarrestin and the character of internalization for the different mutants. Significantly, DOR5A (internalization-deficient) receptors failed to mediate substantial βarrestin translocation while wild-type DOR (internalization-competent) activation caused a pronounced redistribution of βarrestin to the plasma membrane. The results of the present study, combined with these earlier observations of opioid receptor trafficking, clearly suggest that the inhibitory actions of the distal carboxy-tail of DOR and the CB_1 cannabinoid receptor may be a general mechanism of GPCR regulation.

Desensitization of the CB_1 cannabinoid receptor is βarrestin-2-dependent and requires phosphorylation of serines 426 and 430 in the cytoplasmic tail (Jin et al. 1999; Kouznetsova et al. 2002). In fact, truncation of the receptor at residue 460 is without effect on rapid desensitization of CB_1 receptor-mediated activation of inwardly rectifying K^+ channels, suggesting internalization does not contribute to rapid receptor desensitization of these currents (Jin et al. 1999). However, the consequence of carboxy-terminal mutations to the time course of CB_1 receptor-mediated activation of ERK1/2, another important transduction pathway, has not been determined. Therefore we evaluated the kinetics of CB_1 receptor-mediated ERK1/2 activation by the truncation and phosphorylation site mutants. Surprisingly, while the time to peak activation was similar, residual ERK1/2 activity (as measured by its phosphorylation) was evident with protracted stimulation in cells expressing either the truncated receptor or phosphorylation site mutants. These results, coupled with our earlier findings (Roche et al. 1999; Daigle et al. 2008), unequivocally establish that CB_1 receptor internalization is not required for ERK1/2 activation. However, residues within the carboxy-terminus of the CB_1 receptor may be necessary for desensitization of ERK1/2 phosphorylation – a much less rapid process (minutes versus seconds) than GIRK channel desensitization.

In summary, our results suggest that CB_1 receptor endocytosis in HEK293 cells is regulated by a distinct inhibitory mechanism involving the distal carboxy-terminus of the receptor. This process may be a general mechanism of GPCR regulation and modulating this interaction may potentially be a target to attenuate the development of tolerance during prolonged administration of GPCR agonists.

Supplementary Material

Refer to Web version on PubMed Central for supplementary material.

Acknowledgments

This work was supported by DA07278 (T.D.), DA11322 (K.M.) and DA21696 (K.M.). We would like to thank Marc Caron, Jeffrey Benovic and Roger Tsien for βarrestin and RFP constructs, Christopher Kearn and Jim Wager-Miller for help with assay development and constructive discussions and Steven Valm for excellent technical assistance.

Abbreviations

AFU	averaged fluorescence units
cAMP	cyclic-adenosine monophosphate
CB_1R	cannabinoid 1 receptor
CHO	Chinese hamster ovary cells
CP	CP 55,940
GFP	green fluorescent protein
GIRK	inwardly-rectifying K^+ channels
GPCR	G-protein-coupled receptor
GRKs	G-protein-coupled receptor kinases
HBS	Hepes-buffered saline
HEK	human embryonic kidney
HU	HU-210
MAP	mitogen-activated protein
RFP	red fluorescent protein
SR1	SR141716A
WIN	WIN 55,212-2

References

Andersson H, D'Antona AM, Kendall DA, Von Heijne G, Chin CN. Membrane assembly of the cannabinoid receptor 1: impact of a long N-terminal tail. Mol Pharmacol. 2003; 64:570–577. [PubMed: 12920192]

Barak LS, Ferguson SS, Zhang J, Caron MG. A beta-arrestin/green fluorescent protein biosensor for detecting G protein-coupled receptor activation. J Biol Chem. 1997; 272:27497–27500. [PubMed: 9346876]

Bass CE, Martin BR. Time course for the induction and maintenance of tolerance to Delta(9)-tetrahydrocannabinol in mice. Drug Alcohol Depend. 2000; 60:113–119. [PubMed: 10940538]

Berghuis P, Rajnicek AM, Morozov YM, Ross RA, Mulder J, Urban GM, Monory K, Marsicano G, Matteoli M, Canty A, Irving AJ, Katona I, Yanagawa Y, Rakic P, Lutz B, Mackie K, Harkany T. Hardwiring the brain: endocannabinoids shape neuronal connectivity. Science. 2007; 316:1212–1216. [PubMed: 17525344]

Bouaboula M, Poinot-Chazel C, Bourrie B, Canat X, Calandra B, Rinaldi-Carmona M, Le Fur G, Casellas P. Activation of mitogen-activated protein kinases by stimulation of the central cannabinoid receptor CB1. Biochem J. 1995; 312(Pt 2):637–641. [PubMed: 8526880]

Breivogel CS, Childers SR, Deadwyler SA, Hampson RE, Vogt LJ, Sim-Selley LJ. Chronic delta9-tetrahydrocannabinol treatment produces a time-dependent loss of cannabinoid receptors and cannabinoid receptor-activated G proteins in rat brain. J Neurochem. 1999; 73:2447–2459. [PubMed: 10582605]

Breivogel CS, Scates SM, Beletskaya IO, Lowery OB, Aceto MD, Martin BR. The effects of delta9-tetrahydrocannabinol physical dependence on brain cannabinoid receptors. Eur J Pharmacol. 2003; 459:139–150. [PubMed: 12524139]

Campbell RE, Tour O, Palmer AE, Steinbach PA, Baird GS, Zacharias DA, Tsien RY. A monomeric red fluorescent protein. Proc Natl Acad Sci U S A. 2002; 99:7877–7882. [PubMed: 12060735]

Chen Z, Gaudreau R, Le Gouill C, Rola-Pleszczynski M, Stankova J. Agonist-induced internalization of leukotriene B(4) receptor 1 requires G-protein-coupled receptor kinase 2 but not arrestins. Mol Pharmacol. 2004; 66:377–386. [PubMed: 15322228]

Claing A, Laporte SA, Caron MG, Lefkowitz RJ. Endocytosis of G protein-coupled receptors: roles of G protein-coupled receptor kinases and beta-arrestin proteins. Prog Neurobiol. 2002; 66:61–79. [PubMed: 11900882]

Coutts AA, Anavi-Goffer S, Ross RA, MacEwan DJ, Mackie K, Pertwee RG, Irving AJ. Agonist-induced internalization and trafficking of cannabinoid CB1 receptors in hippocampal neurons. J Neurosci. 2001; 21:2425–2433. [PubMed: 11264316]

Daigle TL, Kearn CS, Mackie K. Rapid CB1 cannabinoid receptor desensitization defines the time course of ERK1/2 MAP kinase signaling. Neuropharmacology. 2008; 54:36–44. [PubMed: 17681354]

Derkinderen P, Valjent E, Toutant M, Corvol JC, Enslen H, Ledent C, Trzaskos J, Caboche J, Girault JA. Regulation of extracellular signal-regulated kinase by cannabinoids in hippocampus. J Neurosci. 2003; 23:2371–2382. [PubMed: 12657697]

Gainetdinov RR, Premont RT, Bohn LM, Lefkowitz RJ, Caron MG. Desensitization of G protein-coupled receptors and neuronal functions. Annu Rev Neurosci. 2004; 27:107–144. [PubMed: 15217328]

Hammes SR, Shapiro MJ, Coughlin SR. Shutoff and agonist-triggered internalization of protease-activated receptor 1 can be separated by mutation of putative phosphorylation sites in the cytoplasmic tail. Biochemistry. 1999; 38:9308–9316. [PubMed: 10413505]

Heuser JE, Anderson RG. Hypertonic media inhibit receptor-mediated endocytosis by blocking clathrin-coated pit formation. J Cell Biol. 1989; 108:389–400. [PubMed: 2563728]

Howlett AC, Fleming RM. Cannabinoid inhibition of adenylate cyclase. Pharmacology of the response in neuroblastoma cell membranes. Mol Pharmacol. 1984; 26:532–538. [PubMed: 6092901]

Howlett AC, Barth F, Bonner TI, Cabral G, Casellas P, Devane WA, Felder CC, Herkenham M, Mackie K, Martin BR, Mechoulam R, Pertwee RG. International Union of Pharmacology. XXVII. Classification of cannabinoid receptors. Pharmacol Rev. 2002; 54:161–202. [PubMed: 12037135]

Hsieh C, Brown S, Derleth C, Mackie K. Internalization and recycling of the CB1 cannabinoid receptor. J Neurochem. 1999; 73:493–501. [PubMed: 10428044]

Jin W, Brown S, Roche JP, Hsieh C, Celver JP, Kovoor A, Chavkin C, Mackie K. Distinct domains of the CB1 cannabinoid receptor mediate desensitization and internalization. J Neurosci. 1999; 19:3773–3780. [PubMed: 10234009]

Kearn CS, Blake-Palmer K, Daniel E, Mackie K, Glass M. Concurrent stimulation of cannabinoid CB1 and dopamine D2 receptors enhances heterodimer formation: a mechanism for receptor cross-talk? Mol Pharmacol. 2005; 67:1697–1704. [PubMed: 15710746]

Keren O, Sarne Y. Multiple mechanisms of CB1 cannabinoid receptors regulation. Brain Res. 2003; 980:197–205. [PubMed: 12867259]

Kouznetsova M, Kelley B, Shen M, Thayer SA. Desensitization of cannabinoid-mediated presynaptic inhibition of neurotransmission between rat hippocampal neurons in culture. Mol Pharmacol. 2002; 61:477–485. [PubMed: 11854427]

Lefkowitz RJ. Historical review: a brief history and personal retrospective of seven-transmembrane receptors. Trends Pharmacol Sci. 2004; 25:413–422. [PubMed: 15276710]

Leterrier C, Bonnard D, Carrel D, Rossier J, Lenkei Z. Constitutive endocytic cycle of the CB1 cannabinoid receptor. J Biol Chem. 2004; 279:36013–36021. [PubMed: 15210689]

Leterrier C, Laine J, Darmon M, Boudin H, Rossier J, Lenkei Z. Constitutive activation drives compartment-selective endocytosis and axonal targeting of type 1 cannabinoid receptors. J Neurosci. 2006; 26:3141–3153. [PubMed: 16554465]

Mackie K, Hille B. Cannabinoids inhibit N-type calcium channels in neuroblastoma-glioma cells. Proc Natl Acad Sci U S A. 1992; 89:3825–3829. [PubMed: 1315042]

Mackie K, Lai Y, Westenbroek R, Mitchell R. Cannabinoids activate an inwardly rectifying potassium conductance and inhibit Q-type calcium currents in AtT20 cells transfected with rat brain cannabinoid receptor. J Neurosci. 1995; 15:6552–6561. [PubMed: 7472417]

Martin BR, Sim-Selley LJ, Selley DE. Signaling pathways involved in the development of cannabinoid tolerance. Trends Pharmacol Sci. 2004; 25:325–330. [PubMed: 15165748]

Martini L, Waldhoer M, Pusch M, Kharazia V, Fong J, Lee JH, Freissmuth C, Whistler JL. Ligand-induced down-regulation of the cannabinoid 1 receptor is mediated by the G-protein-coupled receptor-associated sorting protein GASP1. Faseb J. 2007; 21:802–811. [PubMed: 17197383]

McDonald NA, Henstridge CM, Connolly CN, Irving AJ. An essential role for constitutive endocytosis, but not activity, in the axonal targeting of the CB1 cannabinoid receptor. Mol Pharmacol. 2007; 71:976–984. [PubMed: 17182888]

Murray SR, Evans CJ, von Zastrow M. Phosphorylation is not required for dynamin-dependent endocytosis of a truncated mutant opioid receptor. J Biol Chem. 1998; 273:24987–24991. [PubMed: 9737953]

Niehaus JL, Liu Y, Wallis KT, Egertova M, Bhartur SG, Mukhopadhyay S, Shi S, He H, Selley DE, Howlett AC, Elphick MR, Lewis DL. CB1 cannabinoid receptor activity is modulated by the interacting protein CRIP1a. Mol Pharmacol. 2007; 72:1557–1566. [PubMed: 17895407]

Rinaldi-Carmona M, Le Duigou A, Oustric D, Barth F, Bouaboula M, Carayon P, Casellas P, Le Fur G. Modulation of CB1 cannabinoid receptor functions after a long-term exposure to agonist or inverse agonist in the Chinese hamster ovary cell expression system. J Pharmacol Exp Ther. 1998; 287:1038–1047. [PubMed: 9864290]

Roche JP, Bounds S, Brown S, Mackie K. A mutation in the second transmembrane region of the CB1 receptor selectively disrupts G protein signaling and prevents receptor internalization. Mol Pharmacol. 1999; 56:611–618. [PubMed: 10462549]

Rubino T, Forlani G, Vigano D, Zippel R, Parolaro D. Modulation of extracellular signal-regulated kinases cascade by chronic delta 9-tetrahydrocannabinol treatment. Mol Cell Neurosci. 2004; 25:355–362. [PubMed: 15033164]

Smyth EM, Austin SC, Reilly MP, FitzGerald GA. Internalization and sequestration of the human prostacyclin receptor. J Biol Chem. 2000; 275:32037–32045. [PubMed: 10889200]

Tappe-Theodor A, Agarwal N, Katona I, Rubino T, Martini L, Swiercz J, Mackie K, Monyer H, Parolaro D, Whistler J, Kuner T, Kuner R. A molecular basis of analgesic tolerance to cannabinoids. J Neurosci. 2007; 27:4165–4177. [PubMed: 17428994]

Whistler JL, Tsao P, von Zastrow M. A phosphorylation-regulated brake mechanism controls the initial endocytosis of opioid receptors but is not required for post-endocytic sorting to lysosomes. J Biol Chem. 2001; 276:34331–34338. [PubMed: 11443128]

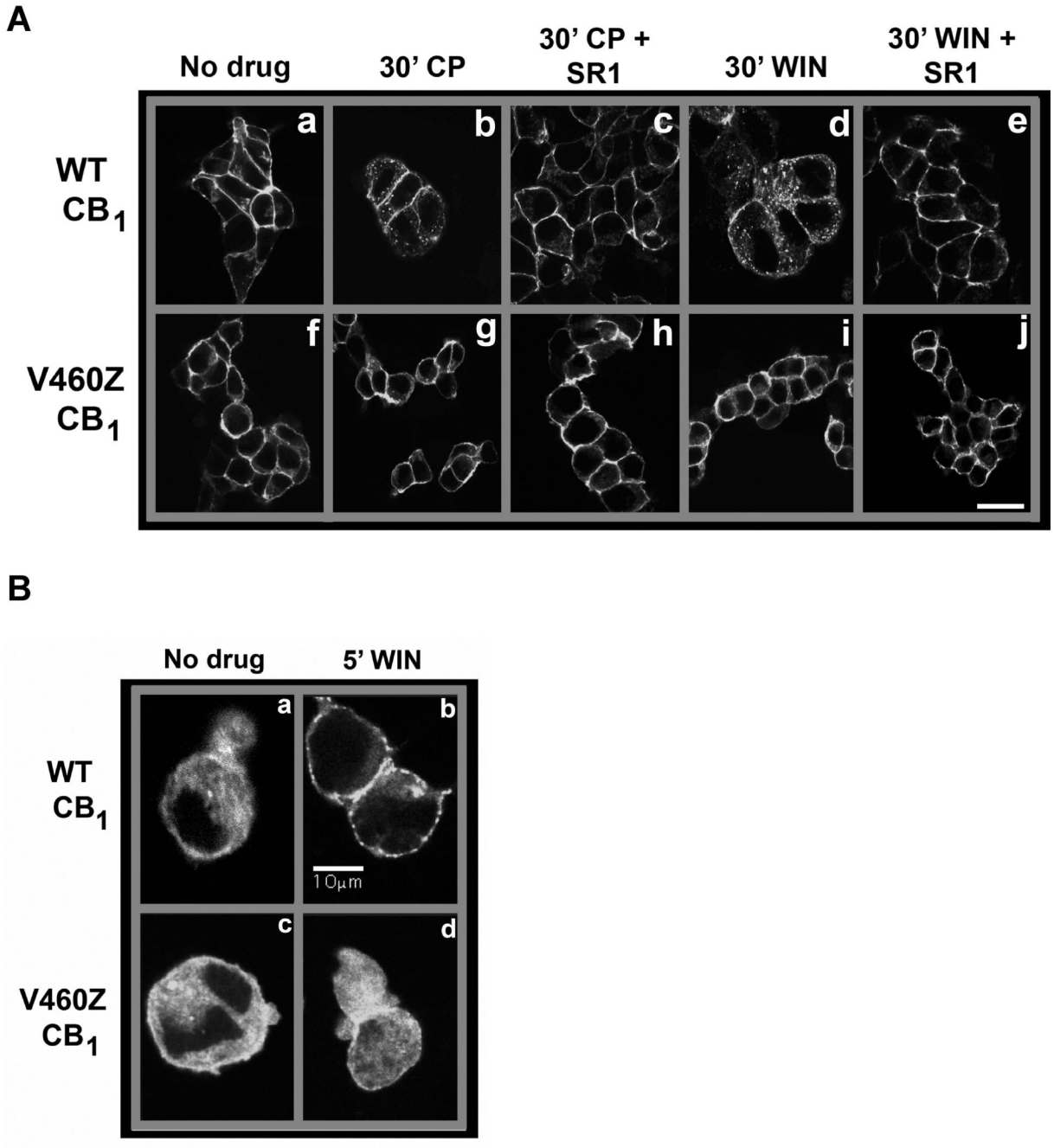

FIG. 1.

V460Z CB_1 receptors do not undergo agonist-induced internalization and fail to recruit βarrestin-2 to the membrane in AtT20 cells. A, Immunocytochemical detection of wild-type and V460Z CB_1 receptors stably expressed in AtT20 cells. Cells were treated with either vehicle (a, f), 1 μM WIN 55,212-2 alone (b, g), 1 μM WIN 55,212-2 in the presence of 1 μM SR141716A (c, h), 100 nM CP 55,940 alone (d, i) or, 100 nM CP 55,940 in the presence of 1 μM SR141716A (e, j) for the indicated times. CB_1 receptors were detected immunocytochemically (see Experimental Procedures). Agonist stimulation resulted in the intracellular accumulation of wild-type CB_1 receptors (b, d). Co-application of SR1 prevented agonist-induced internalization (c, e). In contrast, V460Z CB_1 receptors remained

highly enriched at the cell surface in the presence of agonist (g, i). B, Confocal images of AtT20 cells transiently expressing βarrestin-2-GFP and either wild-type or V460Z CB_1 receptors. βarrestin-2-GFP was detected by its green fluorescence. In unstimulated cells, βarrestin-2-GFP was diffusely present throughout the cell (a, c). CB_1 receptor activation with 100 nM WIN 55,212-2 for 5 min caused a dramatic translocation of βarrestin-2-GFP to the surface with a concomitant decrease in cytosolic fluorescence (b). No translocation was evident in cells expressing V460Z CB_1 receptors (d). Scale bar, 20 μm (A) or 10 μm (B). Images are representative of three independent experiments.

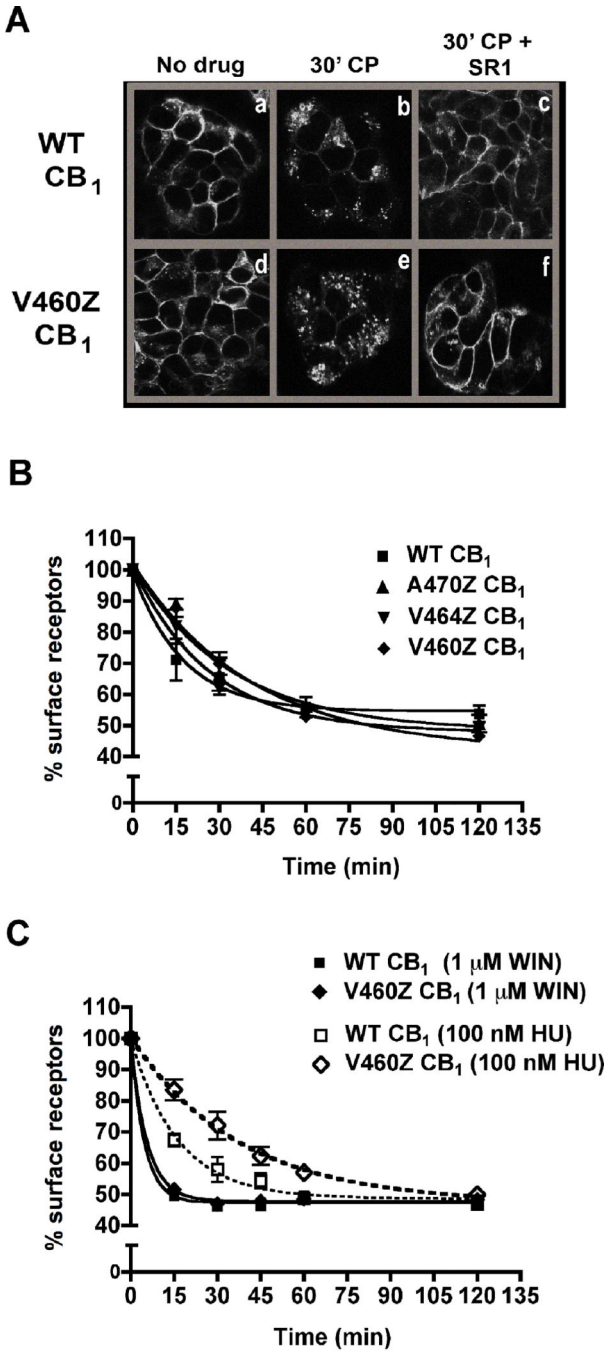

FIG. 2.

Truncation of the last 14 amino acid residues of the CB_1 receptor does not prevent agonist-induced internalization in HEK293 cells. A, Immunostaining of HEK293 cells stably expressing either wild-type or V460Z CB_1 receptors. Cells were treated with vehicle (a, d) or stimulated with 100 nM CP 55,940 alone (b, e) or 100 nM CP 55,940 in the presence of 1 μM SR141716A (c, f) for the indicated times. Both wild-type and V460Z CB_1 receptors were internalized following agonist treatment. Endocytosis was prevented by the addition of SR141716A. Scale bar, 20 μm. Images are representative of a minimum of three independent experiments. B, Quantitative detection of CB_1 receptor removal from the cell surface. HEK293 cells stably expressing either wild-type, A470Z, V464Z or V460Z CB_1

receptors were treated with 100 nM CP 55,940 for times indicated and the time course of receptor internalization was determined (see Experimental Procedures). All of the mutant receptors internalized at a similar rate and to the same extent as wild-type CB_1 receptors. Data are mean ± SEM with n = 15–20 from three to four experiments. C, Time course of wild-type and V460Z CB_1 receptor internalization following 1 μM WIN 55,212-2 (WIN, solid lines) or 100 nM HU-210 (HU, dashed lines) stimulation. Both receptors internalized at a similar rate and extent relative to each other in the presence of either agonist. However, the rate of WIN 55,212-2-induced internalization for both receptors was more rapid than for HU-210-induced endocytosis (see Results). Data are mean ± SEM; n = 6 from three experiments performed in duplicate.

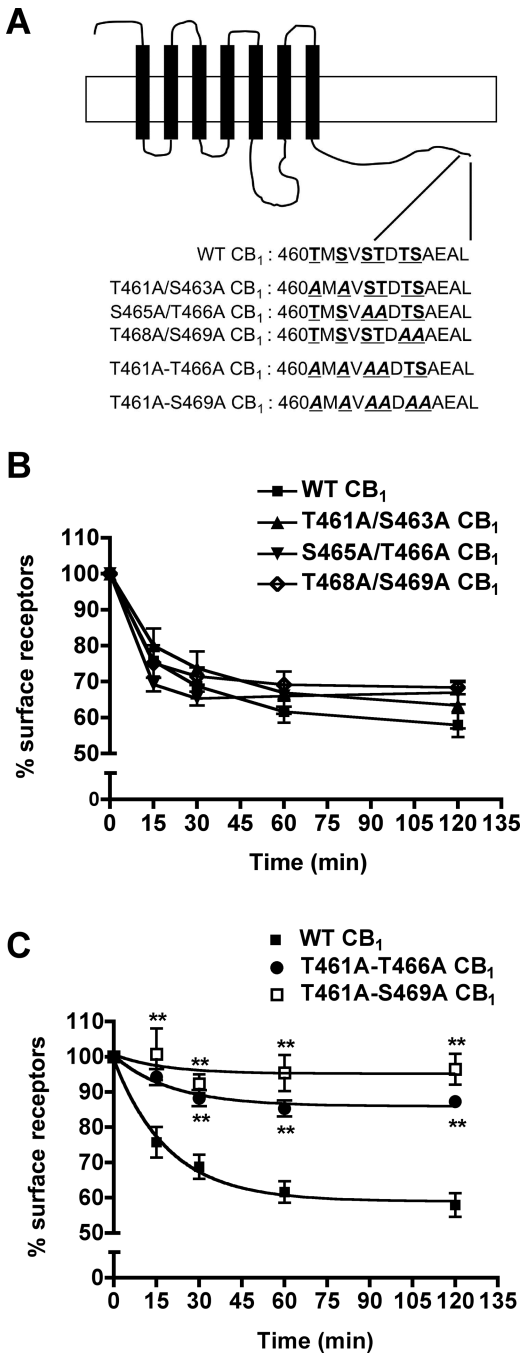

FIG. 3.

Mutation of putative phosphorylation sites in the extreme carboxy-terminus results in a graded effect on the extent of internalization in HEK293 cells. A, Schematic of the rat CB_1 receptor. The serine and threonine residues that were modified for each mutant receptor are italicized. B, Cells expressing either wild-type, T461A/S463A, S465A/T466A, or T468A/S469A CB_1 receptors were stimulated with 100 nM CP 55,940 and the loss of surface receptors with time quantified. The time course of internalization for mutant CB_1 receptors was not significantly different from the wild-type receptor. Data are mean ± SEM; n = 24–34 from four to seven independent experiments. C, Time course of internalization for T461-T466A and T461A–S469A CB_1 receptors. Cells were treated with 100 nM CP 55,940 for

the indicated times. Mutation of four (T461A–T466A) or all six putative phosphorylation sites (T461A–S469A) significantly attenuated the extent of agonist-induced internalization following prolonged drug treatment. Data are mean ± SEM; n = 18–25 from 3–5 experiments. **$p<0.01$ compared with wild-type CB_1 by one-way ANOVA; $p>0.5$ for T461A–T466A CB_1 compared with T461A–S469A CB_1 by one-way ANOVA.

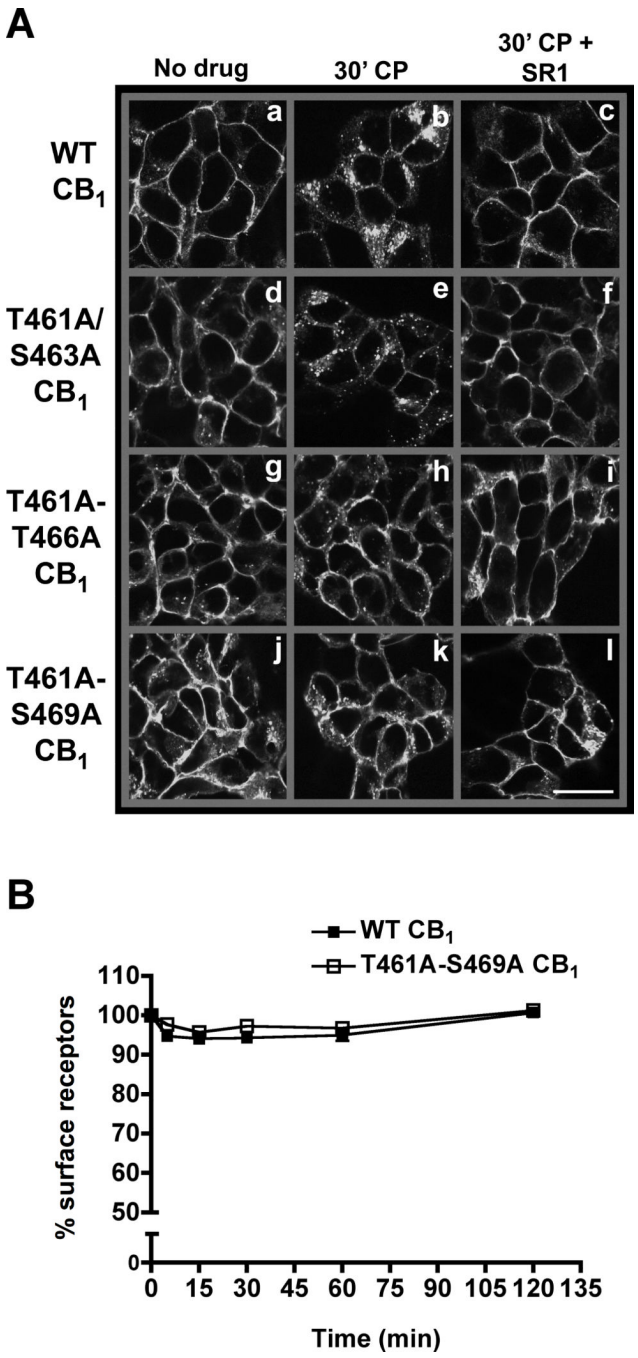

FIG. 4.

Visualization of mutant CB_1 receptor translocation and assessment of constitutive activity. A, Immunostaining of HEK293 cells expressing wild-type, T461A/S463A, T461A–T466A or T461A–S469A CB_1 receptors. Cells were treated with vehicle (a, d, g, j) or stimulated with either 100 nM CP 55,940 alone (b, e, h, k) or 100 nM CP 55,940 in the presence of 1 μM SR141716A (c, f, i, l). Both wild-type and T461A/S463A CB_1 receptors were rapidly internalized following agonist activation, whereas T461A–T466A and T461A–S469A receptors remained on the cell surface. Images are representative of three experiments. Scale bar, 20 μm. B, Receptor trafficking in the presence of SR141716A. Cells were incubated with 1 μM SR141716A and the amount of surface receptors was quantified. SR141716A

treatment did not significantly increase the percentage of wild-type or mutant CB_1 receptors on the cell surface indicating that internal receptors were not constitutively active. Data are mean ± SEM; n = 8–16 for two to four experiments.

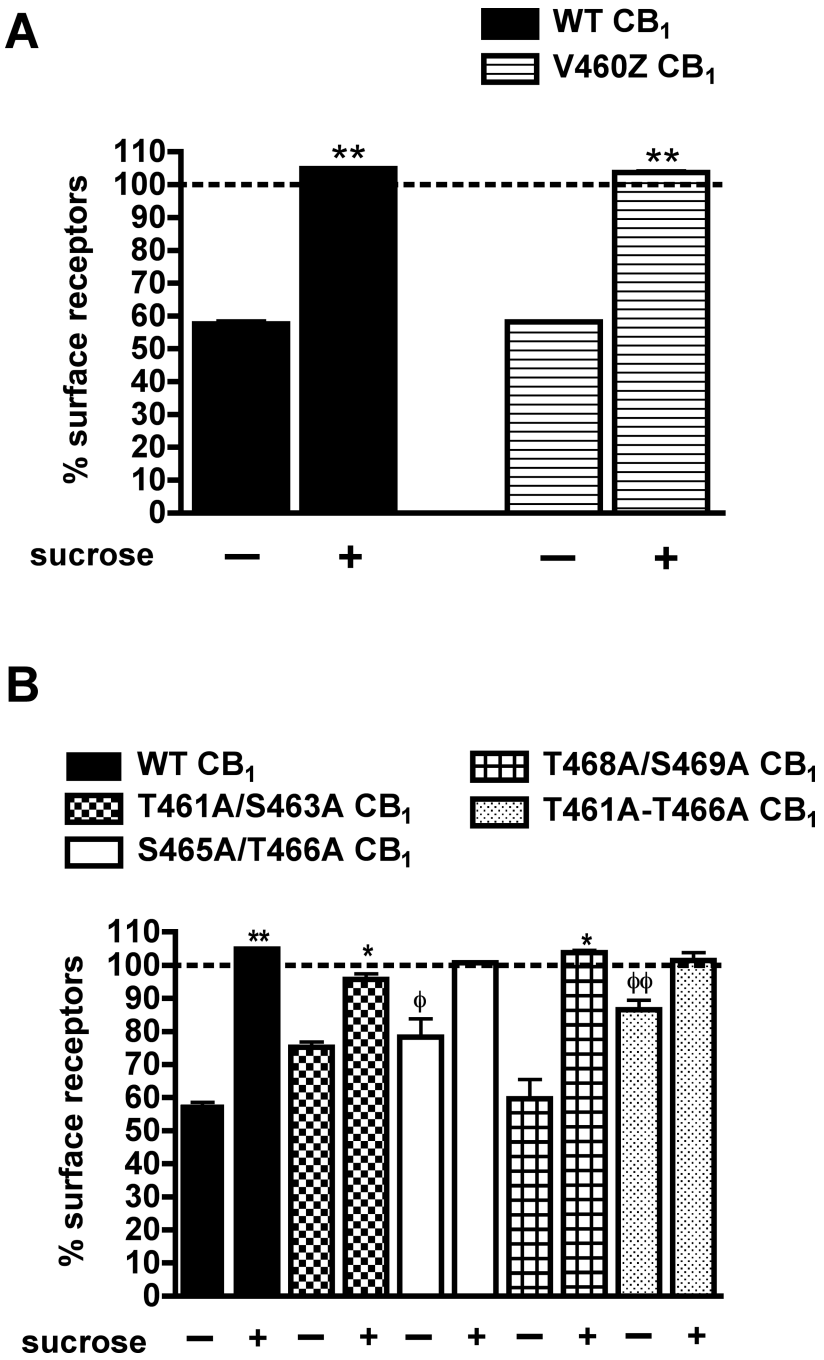

FIG. 5.

Wild-type and mutant CB_1 receptors internalize in a clathrin-dependent manner. A–B, Measurement of CB_1 internalization in the presence or absence of sucrose. Cells were pretreated with a 450 mM sucrose/HBS solution (plus symbols) or HBS alone for 15 min (minus symbols), followed by stimulation with 20 nM CP 55,940 for 45 min. Sucrose pretreatment prevented internalization of wild-type and mutant CB_1 receptors. In the absence of sucrose, CB_1 receptors are internalized to various extents (dependent on the mutation, see above) from the cell surface. Data are mean ± SEM; n = 8 from three experiments. **p<0.01 and *p<0.05 compared with minus sucrose for the individual cell lines and *p<0.01 and **p<0.05 compared with wild-type CB_1 minus sucrose.

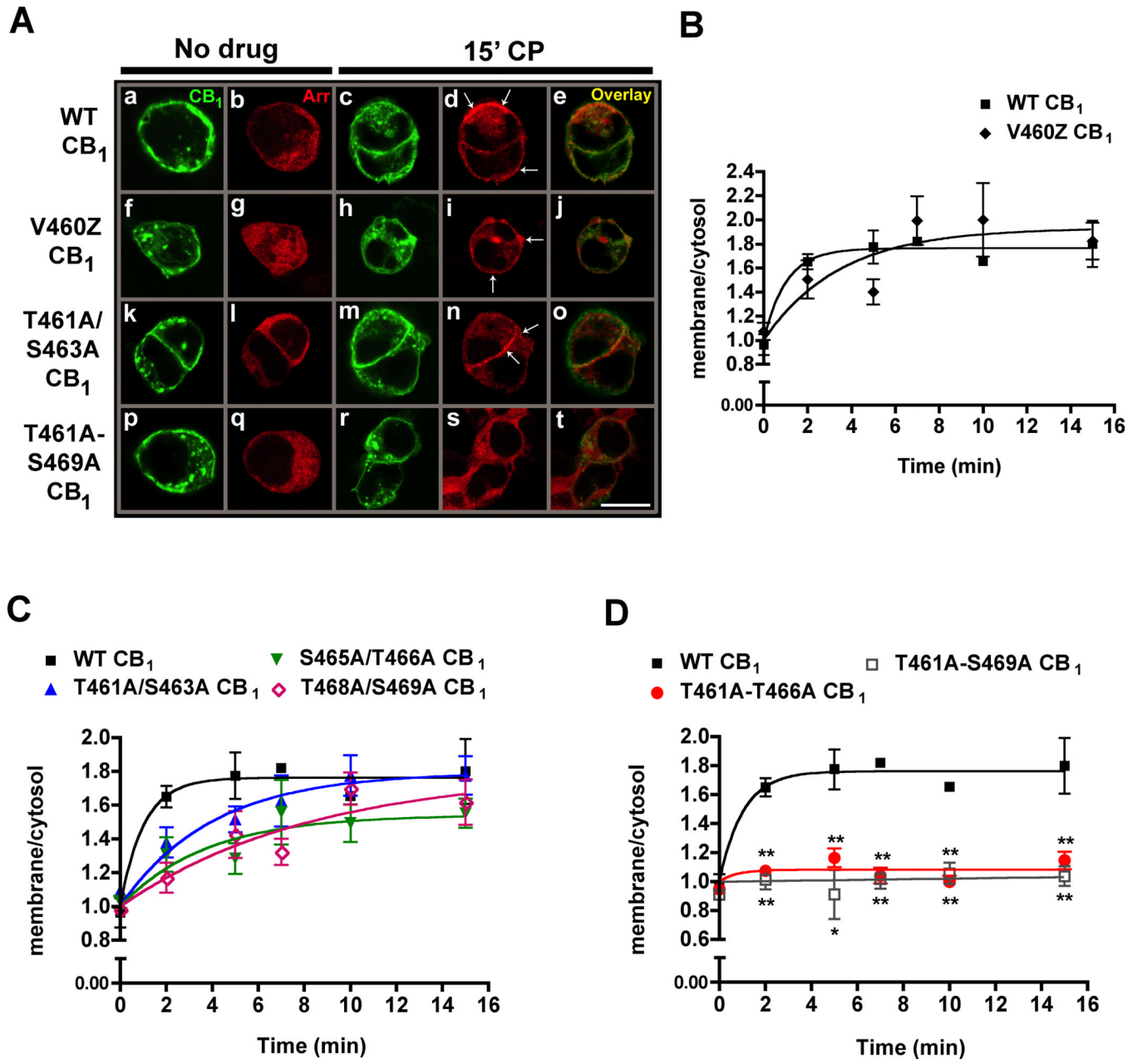

FIG. 6.

Internalization competent CB_1 receptors rapidly recruit βarrestin-2 to the cell surface following agonist activation. A, Images of HEK293 cells transiently expressing βarrestin-2-RFP and either wild-type, V460Z, T461A/S463A or T461A–S463A CB_1 receptors. CB_1 receptors were detected immunocytochemically, while βarrestin-2-RFP was detected by its red fluorescence. Transiently expressed CB_1 receptors are enriched at the cell surface and to a lesser extent, in the cytosol (a, f, k, p). In unstimulated cells, βarrestin-2-RFP was diffusely present throughout the cytosol, and was excluded from the nucleus (b, g, l, q). CB_1 receptor activation with 100 nM CP 55,940 for 15 min caused a profound translocation of βarrestin-2-RFP to the cell surface in cells expressing wild-type, V460Z, or T461A/S463A CB_1 receptors (d, i, n). The overlay shows colocalization of surface CB_1 receptors with clusters of membrane associated Parrestin-2-RFP (e, j, o). No translocation was evident in

cells expressing T461A–S469A CB_1 receptors (s, t). Arrows indicate some regions of βarrestin-2-RFP enrichment at the plasma membrane. Images are representative of three independent experiments. Scale bar, 10 μm. B– D, Quantitation of βarrestin-2-RFP recruitment. Cells were treated with 100 nM CP 55,940 for the indicated times and βarrestin-2-RFP translocation was quantified as described in Experimental Procedures. The ratio of membrane averaged intensity values (AFU; averaged fluorescence unit) to cytosolic averaged intensity values are plotted versus time. Data are mean ± SEM; n = 8–16 cells per time point (for a total of 64–128 defined regions). **$p<0.01$ and *$p<0.05$ compared with wild-type CB_1 receptor.

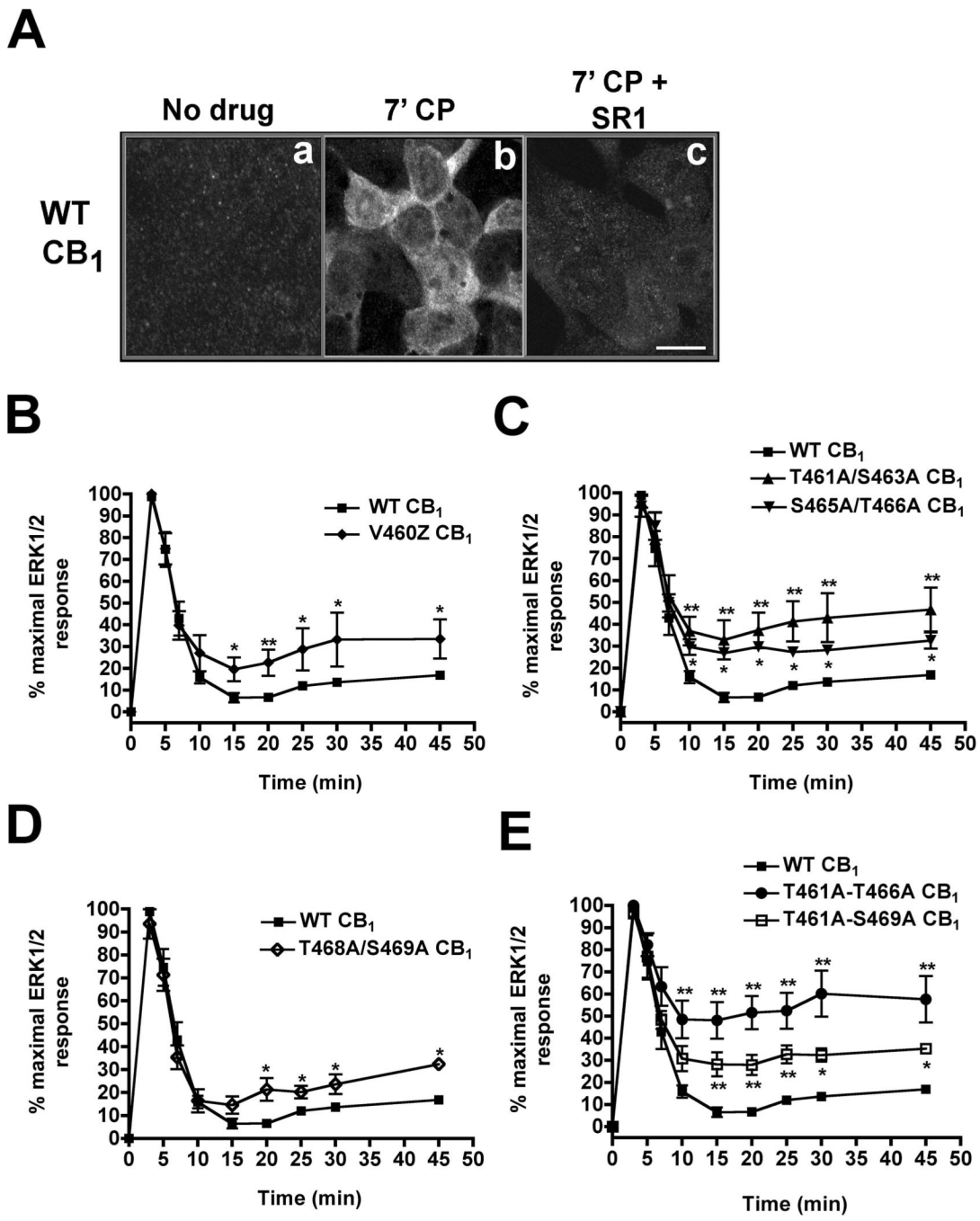

FIG. 7.

The extreme carboxy-terminus of CB_1 contributes to desensitization of MAP kinase signaling. A, Confocal micrographs of phospho-ERK1/2 immunoreactivity. Cells expressing wild-type CB_1 receptors were stimulated with either 100 nM CP 55,940 alone (b) or 100 nM CP 55,940 in the presence of 1 μM SR1 for 7 min (c). B–D, Quantitative detection of phospho-ERK1/2 immunoreactivity (see Experimental Procedures). Time course of ERK1/2 activation in cells expressing either wild-type, V460Z, T461A/S463A, S465A/T466A, T468A/S469A, T461A–T466A and T461A–S469A CB_1 receptors. Cells were treated with 100 nM CP 55,940 for the indicated times. Activation of ERK1/2 in cells expressing mutant CB_1 receptors resulted in a significant increase in ERK1/2 phosphorylation at time points ≥

20 min. Percent maximal ERK1/2 response was calculated by defining basal as the integrated intensity value in vehicle treated cells and setting the maximal peak phosphorylation to 100%. Data are mean ± SEM; n = 6–10 for three to four experiments. **p<0.01 and *p<0.05 compared with wild-type CB_1 by unpaired t-test (panel B) and **p<0.01 and *p<0.05 compared with wild-type CB_1 by one-way ANOVA (panels C–E).